

A CONTACT PROBLEM APPLICATION FOR THE LOCAL BEHAVIOUR OF SOIL PILE INTERACTION

Borana Kullolli*, Henning Stutz†, Jeffrey Bronsert* Paola Dutto* and Matthias Baeßler*

* Bundesanstalt für Materialforschung und Prüfung (BAM)
Unter den Eichen 87, 12205 Berlin
e-mail: borana.kullolli@bam.de web: www.bam.de

† Marine and Land Geomechanics / Geotechnics
Institute of Geo-science Kiel University
Ludewig-Meyn-Str. 10 24118 Kiel

Key words: numerical modeling, contact problem, soil-structure interaction

Abstract: In geotechnical engineering, the main parameter for the performance of structures such as reinforced walls or deep foundations is often the shaft bearing capacity. In numerical analysis, important advancements have been made on studying the behavior of the soil and the retaining structures separately.

The performance of many geotechnical foundation systems depends on the shear behavior at the soil structure interface. For deep foundations, the main component that affects friction is the horizontal earth pressure. When a pile is getting axially loaded, the soil grain network at the interface, starts to move and rearrange. In conditions of axial cyclic loading a contractive behavior of soil can generally be observed as in [1] and [2]. This can be explained by the progressive densification and relaxation of the soil under cyclic shear at the soil pile interface, as well as the local refinement of the grain distribution by grain breakage and rearrangements. As the soil contracts and decreases in volume, the normal stress around the pile surface decreases and the soil pile friction degrades. This can lead to failure of the whole geotechnical foundation system.

The purpose of the work presented in this paper is to analyze locally (at the element level) the contact behavior of a soil-pile contact problem. Therefore, a 2D shear test is modeled using the Finite Element Method. The formulation of a 4 noded zero-thickness interface element of Beer [3] is chosen with a linear interpolation function. Four constitutive contact models adapted for contact problems have been implemented. The simple Mohr-Coulomb [4] and Clough and Duncan [5] models were chosen initially, due to the ease of implementation and few number of parameters needed. After, more complicated models in the framework of elasto-plasticity such as: Lashkari [6] and Mortara [7] were implemented for the first time into the finite element code of the shear test problem. They include other phenomena such as: relative density of soil, the stress level and sand dilatancy. From the results the relation

between shear displacement and shear stress has been deduced. Finally, a discussion of the advantages and the drawbacks during computation of each model is given at the end.

1 INTRODUCTION

In the last century, the number of geotechnical structures has increased significantly. Structures as: reinforced embankments, anchors and deep foundations (offshore and onshore) are becoming more and more present and sophisticated in the civil engineering domain. One of the main parameters of these elements is the shaft bearing capacity [8]. A significant component of the shaft bearing capacity is the shear resistance.

Important advancements have been made on modelling the behavior of the soil and the retaining structures (pile, wall, anchors) separately. The zone in which the soil is attached to a structure is called the interface or contact zone. Many issues and questions arise when it comes to the contact zone between soil and geotechnical element (ex: deep foundation).

The major used numerical technique for modelling the contact behavior in geotechnical engineering is the zero-thickness interface element (e.g. Beer [9] and Goodman [3]). The contact element itself, according to the current deformation and loading, can govern four different states: stick, slip, de-bonding (gap opening) and re-bonding.

The shear behavior of this contact zone is complex due to the composition of materials with a very high stiffness (structure) and in comparison, a very low stiffness (soil). A lot of different experimental studies have indicated the importance of this narrow zone for the global load displacement behavior of geotechnical structures (e.g. for piles [10] and [11]). The before mentioned importance is modelled since a long time using elastoplastic models as the simple Mohr-Coulomb model [4] or more recent elasto-plastic models e.g. Lashkari [6] and Liu [12]. Beside the classical elasto-plastic, generalized plasticity models Liu [13] or hypoplastic models by Stutz et al [14] and [15] exist.

In this paper, the focus was given to the local behavior at the contact zone. An implementation of four different contact constitutive models, two of them for the first time, into a zero-thickness interface element implementation is shown. Because advanced models are seldom implemented into finite-element codes and used for pile-soil interaction analysis. This issue is overcome into this publication. To demonstrate the implementation, a direct interface shear test is modelled using the finite element method. By the results of this direct interface shear test it is shown that the models can be implemented into zero-thickness interface elements even if they have different formulations than the mechanical model used by Goodman [9].

2 CONSTITUTIVE MODELS FOR CONTACT PROBLEMS

When it comes to soil modelling many different constitutive models have been used the theories of elasto-plasticity, hyper-elasticity, hypo-plasticity, generalized plasticity. The majority of this constitutive frameworks have been used for modelling of the interface behavior. All constitutive models treated in the paper are in the framework of elasto-plasticity. The properties and parameters of each model are given in the following subsections.

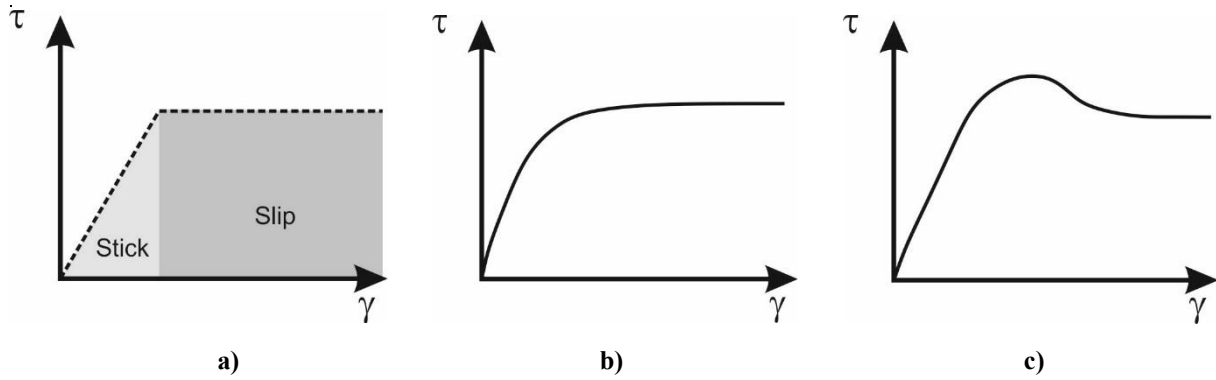


Figure 1: Shear stress vs. shear strain relation for a) Mohr-Coulomb, b) Hyperbolic, c) Mortara and Lashkari

2.1 Mohr-Coulomb model

Mohr-Coulomb model was introduced in 1821 by [4] and since then, further improvement or adaptations for different problems have been made. The formulation of the Mohr-Coulomb model for zero-thickness interface models from [16] is used. As it is a linear-elastic perfectly-plastic model (Figure 1a), after the elastic stress limit is exceed no additional shear stresses are possible. The yield function f is defined as:

$$f = |\tau| + \sigma_n \tan \varphi - c \quad (1)$$

Where τ is the shear stress, σ_n is normal stress, φ is friction angle at interface, and c the cohesion. Vanlangen [4] uses in his model non-associated plasticity. Therefore, the plastic potential g is defined as:

$$g = |\tau| + \sigma_n \tan \psi \quad (2)$$

Where ψ is the dilatation angle. The incremental constitutive relation is obtained as:

$$\dot{t} = D^{ep} \dot{u}^e \quad D^{ep} = D^e - \frac{\alpha}{d} D^e \frac{\partial g}{\partial \sigma_n} \frac{\partial f^T}{\partial \sigma_n} D^e \quad (3)$$

Where \dot{t} denotes the rate of traction vector, D^{ep} is the elasto-plastic matrix, α indicates plasticity if ($\alpha = 1$) or elastic conditions ($\alpha = 0$).

4.2 Hyperbolic model

Clough and Duncan [5] use the nonlinear elasticity model (Figure 1b) from the nonlinear soil model of [4]. To model the non-linear hardening behavior of the interface zone in a Goodman [9] type element. The hyperbola is approximated using some shear test data. The empirical derived equation for the interface behavior is:

$$\tau = \frac{u_s}{a_r + b_r \cdot u_s} \quad (4)$$

Here, τ is the shear stress, a_r , b_r = fitting parameters of hyperbola, u_s = the interface shear displacement.

The model is based on empirical equation converted by linearization to estimate the hyperbolic parameters. Then the straight lines are fitted to the experimental data at the points where the values of shear stress are 70% - 90% of the maximum values.

The shear stiffness depends on normal stress and it is updated at every loop increment.

$$K_s = K_I \gamma_w \left(\frac{\sigma_n}{p_a} \right)^{n_{HY}} \left(1 - \frac{R_f \tau}{\sigma_n \tan \varphi} \right)^2 \quad (5)$$

The shear stress is then calculated as $\tau = K_s * u_s$ and the normal stress σ_n is constant in this model formulation.

4.3 Lashkari model

Here the elasto-plastic model (Figure 1c) according to Lashkari [6] is introduced. The constitutive model relates stress rate vector $[\dot{\sigma}]$ to the velocity vector $[\dot{\Delta}]$ under monotonic shearing. In addition, the model is state dependent and considers the state parameter from Been and Jeffries [17]. By this the parameter calibration is unique for a soil and can be modified to its different states (e.g. loose or dense).

The stress vector $[\sigma]$ and the relative displacement vector $[\Delta]$ are defined as:

$$[\sigma] = \begin{bmatrix} \tau \\ \sigma_n \end{bmatrix} \quad ; \quad [\Delta] = \begin{bmatrix} u \\ v \end{bmatrix} \quad ; \quad [\dot{\Delta}] = [\dot{\Delta}]^e + [\dot{\Delta}]^p \quad (6)$$

Where u, v are the normal and shear displacement respectively. The relative velocity vector is composed out of the elastic and plastic component. For the elastic branch of the velocity vector, the following relation is adapted:

$$[\dot{\sigma}] = \frac{1}{t} [D]^e [\dot{\Delta}]^e \quad (7)$$

Here t represents the thickness and $[D]^e$ is the elastic material matrix. An important parameter is the stress ratio $\eta = \frac{\sigma_n}{\tau}$. It is the main component of model for the yielding plasticity. In case the stress ratio is constant, the behavior remains elastic.

The yield function f is defined as:

$$f = \tau - \eta \sigma_n \quad (8)$$

Finally, the elasto-plastic matrix is given as below:

$$[D]^{ep} = [D]^e - \frac{[D]^e \{R\} \{n\}^T [D]^e}{K_p + \{n\}^T [D]^e \{R\}} \quad (9)$$

Here, $\{n\}$ denotes the yield direction vector, $\{R\}$ is the direction of plastic velocity vector and K_p represents the hardening modulus. For additional details of the model it is referred to Lashkari [6].

4.4 Mortara Model

The elasto-plastic model (Figure 1c) proposed by [7] is an interface constitutive model, which is based on mathematical plasticity formulations. The main advantage of this model is

that can be calibrated with CNL tests, and simulate both Constant Normal Load (CNL) and Constant Normal Stiffness (CNS) boundary conditions in good agreement. In the elasto-plastic theory the stress and strain relation would be:

$$[\dot{\sigma}] = [D]^{ep}[\dot{\epsilon}] \quad (10)$$

The expression for $[D]^{ep}$ is given as:

$$[D]^{ep} = [D]^e - \frac{[D]^e m_M}{H + n^T [D]^e m_M} \quad (11)$$

The component terms of $[D]^{ep}$ are:

$$[D]^e = \begin{bmatrix} K_s^e & 0 \\ 0 & K_n^e \end{bmatrix} \quad m_M = \begin{bmatrix} \frac{\partial g}{\partial \tau} \\ \frac{\partial g}{\partial \sigma_n} \end{bmatrix} \quad n = \begin{bmatrix} \frac{\partial f}{\partial \tau} \\ \frac{\partial f}{\partial \sigma_n} \end{bmatrix} \quad H = -\frac{\partial f}{\partial u_x^p} \quad (12)$$

Where $[D]^e$ is the elastic matrix, K_s^e and K_n^e are the elastic shear and normal stiffness, m_M is the gradient of plastic potential, n is the gradient of plastic surface and H is the hardening modulus. The plastic function of the model was deriving assuming as hardening parameter the normalized shear relative displacement $[\dot{w}_n] = \frac{[\dot{w}^p]}{[w_p^p]}$.

The \dot{w}^p is the time derivative of the plastic shear relative displacement and w_p^p is the shear relative displacement corresponding to the maximum value of the stress ratio. The plastic yield function is given by the expression below:

$$f = \tau - \alpha_M \sigma_n^{\beta_M} = 0 \quad (13)$$

Where α_M is the current value of the hardening rule. More details of the model can be found in [18] and [19]. The plastic potential is given as g is given as:

$$g = \tau - \frac{b}{1+a} \sigma_n \left[1 + a \left(\frac{\sigma_n}{\sigma_c} \right) - \frac{1+a}{a} \right] = 0 \quad (14)$$

Where σ_c is the critical stress. The parameters a and b are the slope and the intercept of the flow rule to the stress ratio η .

3 CONTACT ELEMENT DESCRIPTION

Beside the constitutive models that are necessary, the numerical simulation technique for the discontinuity at the contact is also important. Here, we use the zero-thickness interface, beside this the thin-layer element formulation from Desai [20] and the Mortara [7] method can be used. For the shear test modeled numerically in this paper, the zero thickness element of [9], was used. It has 4 nodes and 8 displacement degrees of freedoms in total. The formulation is derived based on two relative displacements of the continuum element on both sides of the interface. One displacement component is the normal, and the other one is the tangential component to the interface.

Starting from the energy equation and minimizing with respect to nodal point displacements, the element stiffness for the four-nodal point element is indicated in Figure 2.

As the element has zero thickness, the nodes 1,4 and 2,3 have identical coordinates at the beginning of the simulation.

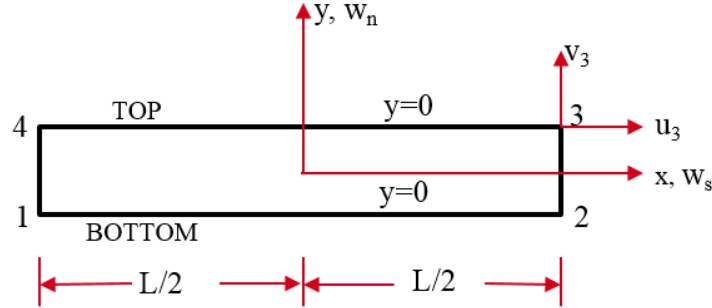


Figure 2: Zero thickness contact element geometry [9]

The vector $[\mathbf{u}]$ contains all nodal displacements in the local coordinate system, where u refers to horizontal displacement and v to vertical displacement. Indexes 1,2,3,4 refer to the node number.

$$[\mathbf{u}] = [u_1 \ v_1 \ u_2 \ v_2 \ u_3 \ v_3 \ u_4 \ v_4] \quad (15)$$

The vector of relative displacements $\{w\}$ is defined as:

$$\{w\} = \begin{Bmatrix} w_s \\ w_n \end{Bmatrix} = \begin{Bmatrix} u_t - u_b \\ v_t - v_b \end{Bmatrix} \quad (16)$$

Where w_s, w_n are tangential and normal relative displacements. u, v are the displacements along x and y axis and t, b = top/bottom segment of the interface. Displacements u, v can be approximated by using standard linear Gaussian interpolation functions $N1, N2$:

$$N1 = \frac{1}{2} - \frac{x}{l} \quad N2 = \frac{1}{2} + \frac{x}{l} \quad (17)$$

$$\begin{Bmatrix} u_t \\ v_t \end{Bmatrix} = \begin{bmatrix} -N1 & 0 & -N2 & 0 & 0 & 0 & 0 & 0 \\ 0 & -N1 & 0 & -N2 & 0 & 0 & 0 & 0 \end{bmatrix} [\mathbf{u}] \quad (18)$$

$$\begin{Bmatrix} u_b \\ v_b \end{Bmatrix} = \begin{bmatrix} 0 & 0 & 0 & 0 & N1 & 0 & N2 & 0 \\ 0 & 0 & 0 & 0 & 0 & 0 & N1 & 0 \end{bmatrix} [\mathbf{u}] \quad (19)$$

The strain displacement matrix $[B]$ is given as:

$$[B] = \begin{bmatrix} -N1 & 0 & -N2 & 0 & N1 & 0 & N2 & 0 \\ 0 & -N1 & 0 & -N2 & 0 & N1 & 0 & N2 \end{bmatrix} \quad (20)$$

The strain energy U can be calculated as:

$$U = \frac{1}{2} [u]^T \int_{-l/2}^{l/2} [B]^T [D^e][I][B] dx \quad (21)$$

From the Eq. (21) the stiffness matrix K can be calculated:

$$K = \int_0^l [B]^T [D^e][I][B] dx \quad (22)$$

The strain matrix:

$$\varepsilon = [B] [u] \quad (23)$$

The assumption of Goodman et al. [9] is to have a continuous displacement field that leads to a continuous stress field through the length l . For an elastic behavior, the stress as obtained:

$$\sigma = [D^e] [\varepsilon] \quad (24)$$

In the group of zero thickness family can be found more advanced contact elements which take in consideration more complicated phenomena. Cerfontaine et al [21] proposed a 3D hydro-mechanical coupled element. The element belongs to the zero-thickness formulation and the contact constraint is ensured by the penalty method. Fluid flow is discredited through a three-node scheme, discrediting the inner flow by additional nodes. The element can reproduce stick, slip, bonding, de-bonding degrees of freedom. Stutz et al [22] proposed an extended zero thickness element which reproduces the gap opening for cohesive soils. The interface element consists in a 16-node element with an isoparametric formulation.

4 NUMERICAL MODEL

4.1 Direct shear test model description

In order to study the local soil-pile interface behavior, a direct shear test was modeled numerically. The problem was treated with a 2D plane strain model. The model consists of two different domains: soil (upper part) and solid (lower part) as shown in Figure 3.

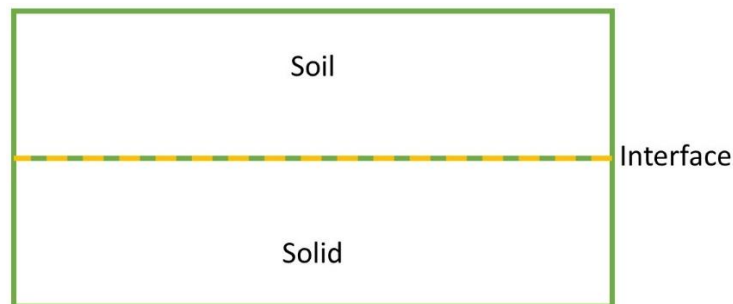


Figure 3: Shear test geometry

On the structure/solid block, zero displacement both in vertical and horizontal direction were imposed (Figure 4). The normal pressure $p_n = 100\text{kPa}$ was imposed on top of the soil part and a shear displacement $u_s = 1\text{ cm}$ was imposed on the left side. The continuum behavior of the solid and the soil domain are considered purely elastic. In this study only the non-linear behavior of the contact zone is studied. The dimensions of each block are $25\text{cm} \times 5\text{ cm}$. The model has in total 20 elements. Each block is divided in 8 quadrilateral elements with 4 nodes and the contact area has 4 zero thickness elements as in [3] also with 4 nodes.

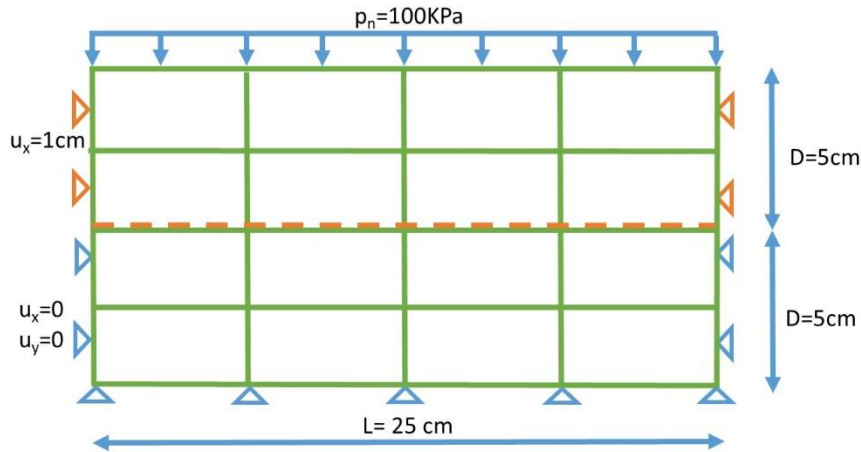


Figure 4: Shear test dimensions and boundary conditions

4.2 Results and discussion

For each constitutive model the relation between shear stress and shear strain is plotted in Figure 5. Even though the continuum material properties and boundary conditions remained the same, different interface models lead to different stress-displacement results. The parameters for each model can be found in the Appendix A.

The Mohr-Coulomb contact model is advantageous in terms of computational effort, and it has only four parameters to consider. Being a bilinear model, has the disadvantage that once it reaches the maximal stress limit, no other additional stress is captured. The general behavior of this model does not include advances for softening and hardening behavior.

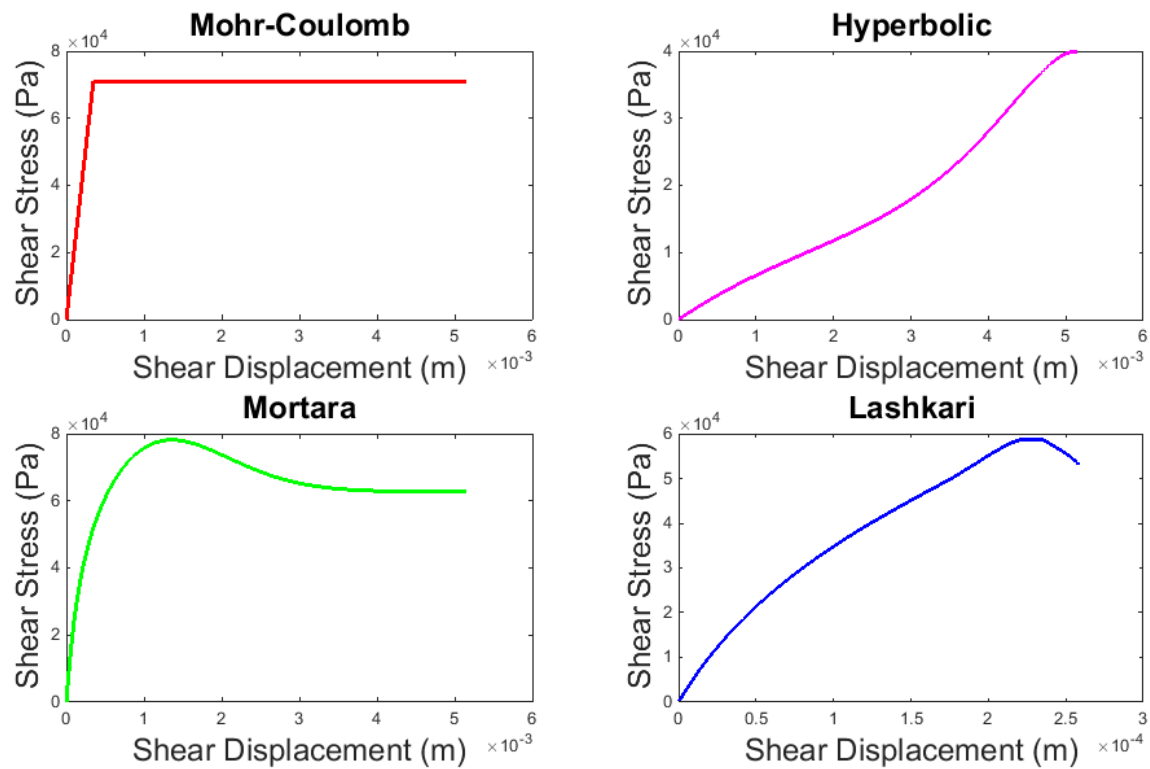
The hyperbolic model is very sensitive to any change of parameters. The displacement increment needs to be very small and having consequently many time steps.

The model from Lashkari [6] model involves 11 parameters. It does not converge until the end, but it is possible reach the peak value. The problem starts to appear when the softening behaviour should appear.

Mortara's model [7] converges until the last step and it reproduces well hardening and softening behavior. The only drawback is the high number of parameters (15).

The comparison of all different implementation is not the aim of the paper, however it is shown that the implementation of advanced interface models is possible and successful. However differences in the achieved accuracy and computational robustness are obvious. A

comparison of values can not be done due to the differences parameter sets which was used in the simulations. The global behaviour of shear test under normal pressure loading and shear displacements is given in Figure 6 using Mortara model. The global behaviour of the direct interface test simulation in terms of shear stress deformed shape is presented in Figure 6 and shows the expected results.



[21]

Figure 5: Results from the numerical model for each constitutive model

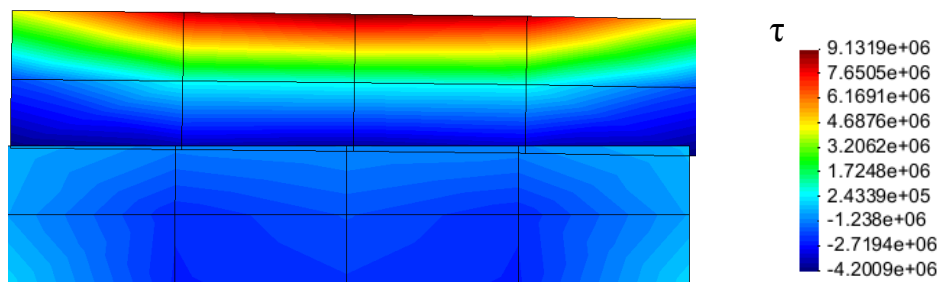


Figure 6: Gid post-process results

5 CONCLUSIONS

- Contact elements are an important tool to study the behavior of shaft friction. Along with an adequate constitutive model, they are able to model numerically the phenomena that are important in the contact area between soil and pile.
- Preliminary results on monotonic loading showed that Mortara's model produces reasonable results compared to the other model. Nevertheless, the high number of parameters makes it challenging to use the model for different soils.
- The study of the different models helps to identify issues and challenges for future work about the implementation and usage of the different models. In addition, this helps for model improvement and development of the models.

REFERENCES

- [1] Boulon M, Foray P. Physical and numerical simulation of lateral shaft friction along offshore piles in sand. Proc 3rd International Conference on Numerical methods in offshore piling, Nantes, France 1986. p. 127-47.
- [2] Dejong JT, White DJ, Randolph MF. Microscale observation and modeling of soil-structure interface behavior using particle image velocimetry. *Soils and Foundations*. 2006;46:15-28 DOI: 10.1002/nme.1620210402.
- [3] Beer G. An isoparametric joint/interface element for finite element analysis. *International journal for numerical methods in engineering*. 1985;21:585-600 DOI: 10.1002/nme.1620210402.
- [4] de Coulomb CA. *Théorie des machines simples: en ayant égard au frottement de leurs parties et à la roideur des cordages*: Bachelier; 1821.
- [5] Duncan J, Clough G. Finite element analysis of retaining wall behaviour. *Journal of Geotechnical Engineering, ASCE*. 1971;97:232-40
- [6] Lashkari A. Prediction of the shaft resistance of nondisplacement piles in sand. *International Journal for numerical and analytical methods in geomechanics*. 2013;37:904-31
- [7] Mortara G. An elastoplastic modelling sand structure interface behaviour under monotonic and cyclic loading [PhD] 2003.
- [8] Jardine R, Standing J. Pile load testing performed for HSE cyclic loading study at Dunkirk, France: Health and Safety Executive; 2000.
- [9] Goodman RE, Taylor RL, Brekke TL. A model for the mechanics of jointed rocks. *Journal of Soil Mechanics & Foundations Div*. 1968
- [10] Lehane BM, White DJ. Lateral stress changes and shaft friction for model displacement piles in sand. *Canadian Geotechnical Journal*. 2005;42:1039-52 DOI: 10.1139/T05-023.
- [11] Tehrani F, Han F, Salgado R, Prezzi M, Tovar R, Castro A. Effect of surface roughness on the shaft resistance of non-displacement piles embedded in sand. *Géotechnique*. 2016;2:1-15 DOI: 10.1680/jgeot.15.P.007
- [12] Liu H, Song E, Ling HI. Constitutive modeling of soil-structure interface through the concept of critical state soil mechanics. *Mechanics Research Communications*. 2006;33:515-31 DOI: 10.1016/j.mechrescom.2006.01.002.

- [13] Liu J, Zou D, Kong X. A three-dimensional state-dependent model of soil–structure interface for monotonic and cyclic loadings. *Computers and Geotechnics*. 2014;61:166-77 DOI: 10.1016/j.compgeo.2014.05.012.
- [14] Stutz H, Mašin D. Hypoplastic interface models for fine-grained soils. *International Journal for numerical and analytical methods in geomechanics*. 2017;41:284-303 DOI: 10.1002/nag.2561.
- [15] Stutz H, Mašin D, Wuttke F. Enhancement of a hypoplastic model for granular soil–structure interface behaviour. *Acta Geotechnica*. 2016;11:1249-61 DOI: 10.1007/s11440-016-0440-1.
- [16] Vanlangen H. Numerical analysis of soil-structure interaction. 1991
- [17] Been K, Jefferies MG. A state parameter for sands. *Géotechnique* 1985. p. 99-112.
- [18] Ghionna VN, Mortara G. An elastoplastic model for sand–structure interface behaviour. *Géotechnique*. 2002;52:41-50 DOI:10.1680/geot.2002.52.1.41.
- [19] Mortara G. An elastoplastic model for sand-structure interface behaviour under monotonic and cyclic loading: Ph. D. Thesis. Technical University of Torino; 2001.
- [20] Desai C, Zaman M, Lightner J, Siriwardane H. Thin-layer element for interfaces and joints. *International Journal for numerical and analytical methods in geomechanics*. 1984;8:19-43
- [21] Cerfontaine B, Dieudonné A-C, Radu J-P, Collin F, Charlier R. 3D zero-thickness coupled interface finite element: formulation and application. *Computers and Geotechnics*. 2015;69:124-40 DOI: 10.1016/j.compgeo.2015.04.016.
- [22] Stutz H, Wuttke F, Benz T. Extended zero-thickness interface element for accurate soil–pile interaction modelling. *Numerical Methods in Geotechnical Engineering*. 2014:283 DOI: 10.1201/b17017-52

APPENDIX A

Mohr-Coulomb			
Parameter	Definition	Unit	Value
E	Young Modulus	MPa	60
ν	Poisson ratio	-	0.35
φ	Interface friction angle	-	35
c	Cohesion	KPa	1

Hyperbolic			
Parameter	Definition	Unit	Value
γ_w	Unit weight of water	N/m^3	10000
K_I	Dimensionless stiffness number	-	70000
n_{HY}	Stiffness exponent	-	0.75
R_f	Failure ratio	-	0.92
φ	Interface friction angle	°	35

Mortara			
Parameter	Definition	Unit	Value
K_{s0}^e	Elastic tangential stiffness	MPa	500e6
K_{n0}^e	Elastic Normal stiffness	MPa	585e6
A_0	Initial dilatancy constant	-	11
A_{1L}	Intermediate dilatancy constant	-	0.85
h_0	Plastic hardening modulus constant	-	0.35
M_L	Critical stress ratio	-	0.638
e_0	Initial void ratio	-	1.01
λ_L	Critical state line location in $e-\ln\sigma_n$	-	0.09
n^b	Influence of interface state on peak stress ratio	-	1.15
n^d	Influence of state on phase transformation	-	0.73
t	thickness	m	0.003

Lashkari			
Parameter	Definition	Unit	Value
K_n^e	Elastic normal stiffness	Pa/m	1.0e10
C_k	Ratio between normal and shear stiffness	-	1
α_p	Maximum value of hardening value	$PA^{1-\beta M}$	2.68
α_c	Asymptotic value of the hardening function	$PA^{1-\beta M}$	2.15
ξ_M	ω_p paramater	PA^{-1}	3.68e-9
ζ	ω_p paramater	m	7.26e-5
μ_M	d_{max} paramater	PA^{-1}	2.171e-7
v_d	d_{max} paramater	-	0.24
ρ_M	Ratio between stress ratios for d=0 for hardening or softening condition	-	0.550
β_M	Exponent of plastic functions	-	0.9
ω	Hardening model parameter	-	235.6
ψ	Hardening model parameter	-	0.16